International Journal of Science and Research (IJSR)
ISSN: 2319-7064
SJIF (2022): 7.942

Classification of Oral Lesions using Deep Learning: A Retrospective Study

Hemashree H C[1], Pradeep N[2]

[1] Department of Information Science and Engineering, Bapuji Institute of Engineering and Technology, Davangere, affiliated to Visvesvaraya Technological University, Belagavi, Karnataka, India

[2] Department of Computer Science and Engineering, Bapuji Institute of Engineering and Technology, Davangere, affiliated to Visvesvaraya Technological University, Belagavi, Karnataka, India

Abstract: ***The sixth most frequent cancer with a high death rate from disease - related causes is oral cancer. The main cause is that almost two thirds of patients receive a cancer diagnosis later in the disease's progression. Oral potentially malignant disorders (OPMDs) are observable alterations in the oral mucosa that occur before most oral malignancies. In 88% of cases, early detection of OPMDs can prevent the development of malignancy. The use of artificial intelligence (AI) in medicine, particularly oncology, has grown in popularity since it has shown useful in diagnosing and predicting the prognosis of cancer. This study uses a dataset of clinically annotated photographic pictures to identify oral precancerous and cancerous lesions and distinguish them from normal mucosa using pre - trained convolutional neural networks (CNNs). Clinical images of patients with oral squamous cell carcinoma and OPMDs were used in this investigation. Photographs of the normal oral mucosa were compared with these images for analysis. Image categorization was done by transfer learning with different CNN architectures that had already been trained. Regarding performance against other models, VGG19 performed well in the current investigation.***

Keywords: Oral cancer; Artificial intelligence; Diagnosis; Image classification; Cancer prognosis.

1. Introduction

All malignant lesions affecting the lip, buccal mucosa, hard palate, floor of the mouth, gingiva, and anterior two thirds of the tongue are included in the category of oral cancer. [1] With significant rates of morbidity and mortality due to the disease, it is the sixth most frequent cancer in the world. [1] A worldwide health concern, according to Global Cancer Statistics 2020, there were 377, 713 cases reported and 177, 757 cases of death from the disease in 2020. [2] The general death rate has not decreased despite the development of several new treatment methods, and the prognosis is still dire, with a survival rate over the course of five years of 28–67%. [3] The main cause of the above is that almost two thirds of patients receive a cancer diagnosis later in life. [4] Healthcare professionals' understanding, public awareness, and a lack of early screening are among the likely reasons for the delayed diagnosis. [4]

Oral potentially malignant diseases (OPMDs) are visible alterations in the oral mucosa that occur before most cases of oral cancer. [4, 5] Usually, these take the form of chronic ulcerations, red patches, non - scrapable white plaques, and mixed red and white areas. [1] In 88% of cases, early detection and treatment of OPMDs can prevent the development of malignancy. Additionally, a lower death rate and a delayed stage of the disease can result from early detection of malignant lesions. [4 - 6] Despite the fact that the oral cavity is much easier to examine thoroughly than other organs, a traditional examination may not always be able to distinguish between benign and OPMD lesions. [7] Therefore, developing an affordable and sensitive screening diagnostic tool is imperative given the rising incidence of oral cancer, particularly in low - income nations. [4] Using technology would be a workable and long - lasting answer. When compared to traditional inspection and analysis, prior research has demonstrated good agreement with photos when employing telemedicine and WhatsApp for clinical diagnosis and remote screening of OPMDs. [8–10] When identifying OPMDs and the malignant lesion, it can be very helpful to incorporate an automated detection system that is connected to telemedicine tools through artificial intelligence (AI). [4]

Artificial intelligence has become more and more common in the medical industry, particularly in oncology, over the past ten years. It has demonstrated effectiveness in the identification and prognostication of cancer. Artificial Intelligence mimics human cognitive processes on robots. [3] Convolutional neural networks (CNNs) like Alex Net, Google Net, Mobile Net, VGG19, VGG16, InceptionV3, ResNet50, and Squeeze Net architecture have been used in studies to diagnose and classify skin malignancies in addition to lung, breast, and colon cancers, with encouraging results. [11–23] In addition, deep learning methods have shown superior to human specialists in spotting minute visual patterns in pictures. [3, 13] A small number of studies have created AI - based algorithms for the diagnosis of Oral Squamous Cell Carcinoma (OSCC) in the literature; the majority of these studies use standardized images, such as images from multidimensional hyperspectral imaging, laser endomicroscopy imaging, computed tomography imaging, histology images, Raman spectra images, and computed tomography imaging. [18] Nonetheless, only a small number of research have used photographic images [7, 19–23], and most of them have concentrated on diagnosing particular kinds of oral lesions. In order to distinguish oral pre - cancerous (perhaps malignant) and cancerous lesions from normal mucosa, a collection of clinically annotated photographic pictures was utilized in the feasibility study. Pre - trained convolutional neural networks were constructed for this purpose.

2. Methodology

2.1 Data collection

Clinical oral photos were retrospectively gathered for this study from the Department of Oral Medicine and Radiology's and the Department of Oral Pathology's archives. The photos that were recovered included normal mucosa, oral lesions that could turn cancerous, and cases of OSCC that were confirmed by biopsy. photos of the same lesion with varying angulations and orientations, photos with blurriness, and images with shadows of other oral structures were not included in the study sample. The related pathologic report resulted to the labels "normal mucosa, " "OPMD, " and "OSCC" being applied to the pictures. The photos were manually cropped and resized because they were shot at various angles and magnifications. The photos' brightness, saturation, and contrast, however, were all left unaltered. After receiving approval from the Institutional Ethics Committee, the study was carried out. A total of 2000 photos were utilized, consisting of 615 OSCC images, 650 OPMD images, and 735 normal images.

2.2 Method

Image classification was carried out by transfer learning with different pre - trained CNNs. This method makes it easier to use the knowledge that pre - trained CNNs—which are trained on a vast amount of non - medical data—have acquired. As seen in Fig.1, the top levels of the pre - trained CNNs were deleted and new layers added in their place. After freezing the bottom layers, freshly added layers were adjusted with a fresh dataset until the system performed at its best. InceptionV3, ResNet50, VGG19, VGG16, and Mobile Net—pre - trained CNN architecture—were taken into consideration for transfer learning experiments. These CNNs' model summaries are displayed in Figs. S1 through S5.

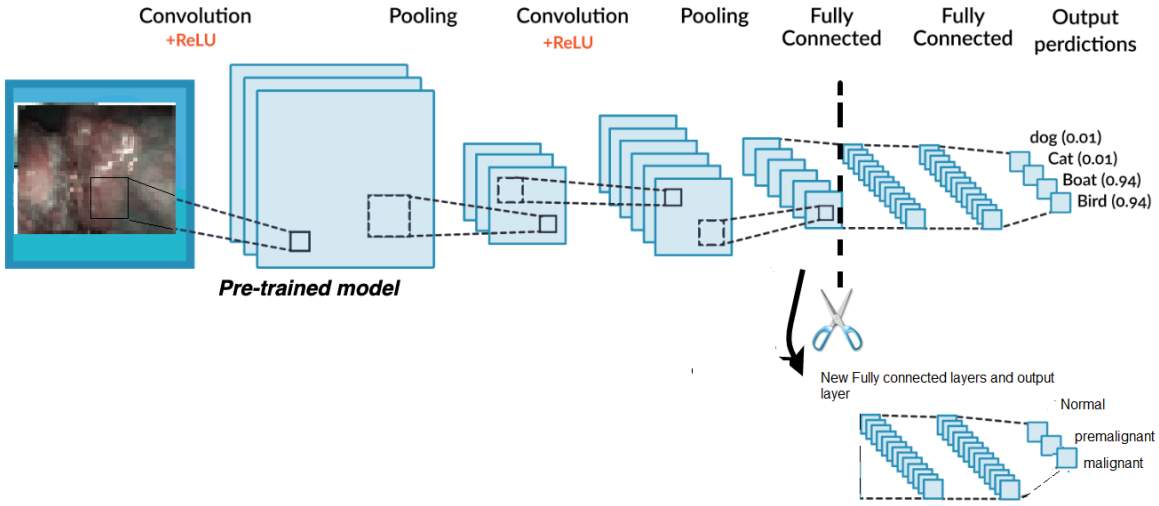

Figure 1: Image categorization using the pre - trained CNN through transfer learning

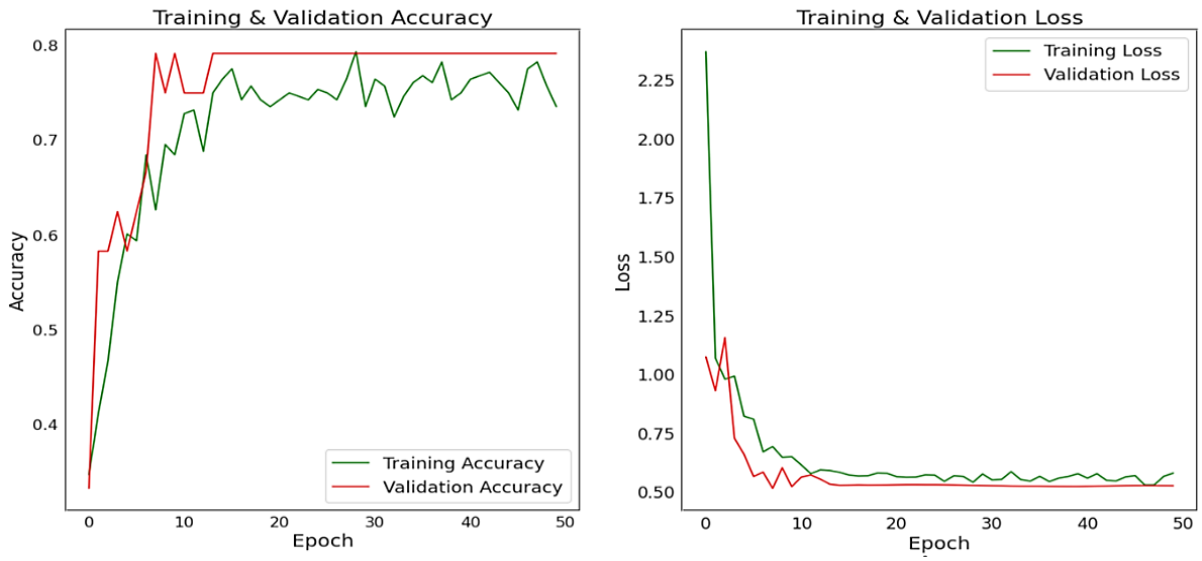

(a) (b)

Figure 2: VGG19 Training and Validation for each epoch (a) Model accuracy (b) Model loss.

The ImageNet dataset, which contains 1.2 million photos divided into 1, 000 classes, served as the training material for all of these CNNs. [24] These CNNs' last dense layer was swapped out with a new dense layer with three neurons, the number of which matched the number of classes in the application under consideration.75% of the data were used for testing and validation, while the remaining 85% were used to train the CNNs. Random flipping, image zooming, and image

rotation were applied to enhance the training images. CNNs were trained for 50 epochs with a learning rate of 0.001 and a batch size of 16. These CNNs' performances were compared, and the network with the best results was chosen.

3. Results and Discussion

A machine equipped with a Tesla 1xK80 graphics card was used for the experimentation. CNN's training was carried out with Python3 Tensor flow version 1.15.2 in Google Colab. Table 1 lists the classification accuracies for test images of several pre - trained networks.

Table 1: Classification accuracies of different pre - trained models

Pre - trained CNN	Accuracy
VGG19	76%
VGG16	72%
Mobile Net	72%
InceptionV3	68%
ResNet50	36%

Among the networks, VGG19 has the highest accuracy at 76%. Fig.2 displays a visualization of the training and validation accuracy and loss for each VGG19 epoch. It is evident from the VGG19's training and validation learning curves (Fig.2) that the model learns well because there is little difference between the training and validation loss curves. Table 2 lists the VGG19 per - class basis classification report. The precision, recall, and F1 - score classification metrics are displayed by class in Table 2. The precision of CNN is its ability to classify a normal image as either pre - cancerous or malignant. Recall shows how well a classifier can locate every positive case. The F1 - score indicates how accurate positive forecasts are. Support indicates the number of instances utilized for testing under each class.

Table 2: VGG19 architecture categorization report on a per - class basis

Class	Precision	Recall	F1 - Score	Support
Malignant	0.6	0.43	0.5	7
Normal	0.9	1	0.95	9
Pre - malignant	0.7	0.78	0.74	9

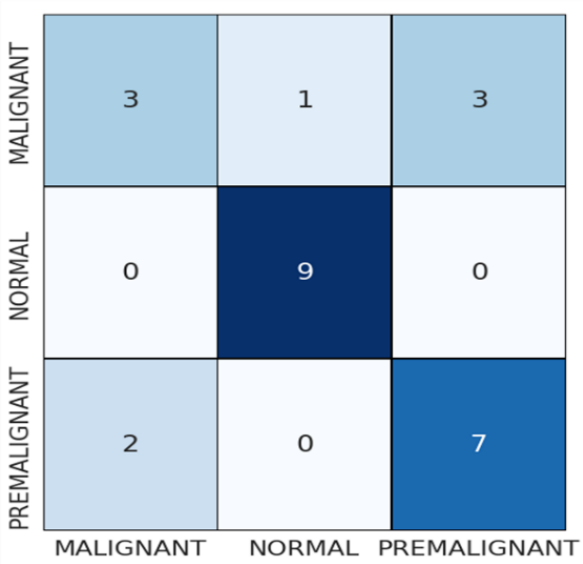

Figure 3: Confusion matrix for VGG19 architecture.

The performance of a CNN can be tabulatedly visualized using a confusion matrix (Fig.3). The comparison between the actual and anticipated classes is obtained using it. Table 2 shows that there are seven images (shown by support) in the malignant class. Looking at the first row of the confusion matrix, three of the seven cancerous images were accurately categorized as such, one as normal, and three as pre - malignant.

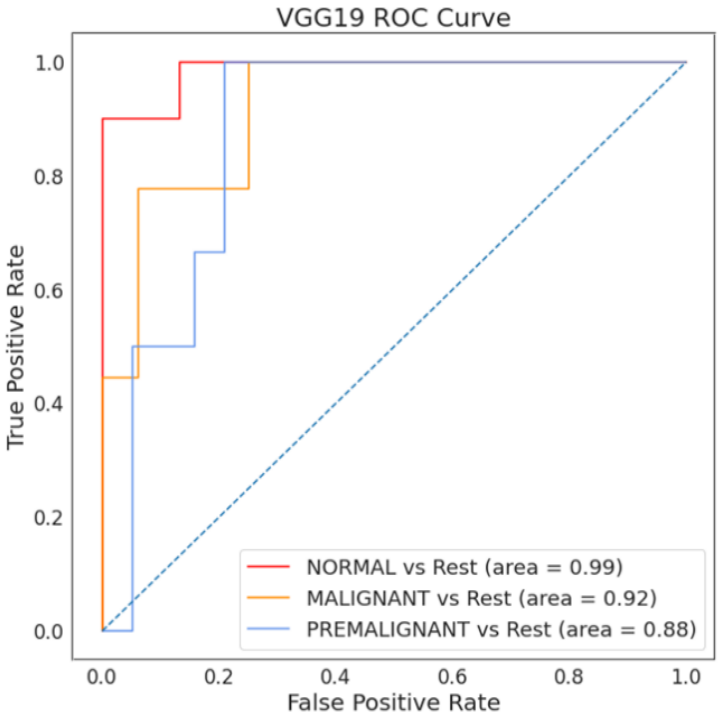

Figure 4: ROC curve of VGG19 architecture over its operating range

Figure 4 displays a plot of the false positive rate (x - axis) against the true positive rate (y - axis) for a number of potential VGG19 threshold values between 0.0 and 1.0. This is known as the receiver operating characteristic (ROC) curve. The classifier's performance can be evaluated across its whole operational range using ROC curves. The area under the curve (AUC) is the most commonly used metric. AUCs of 0.5 show no discrimination, 0.7 to 0.8 are acceptable, 0.8 to 0.9 are exceptional, and greater than 0.9 are exceptional. Fig.5 displays a visualization of the training and validation accuracy and loss for the VGG16 architecture for each epoch.

The training and validation loss curve gaps of VGG16 exhibit an approximate larger gap than VGG19, as can be seen from the learning curves for training and validation (Fig.5).

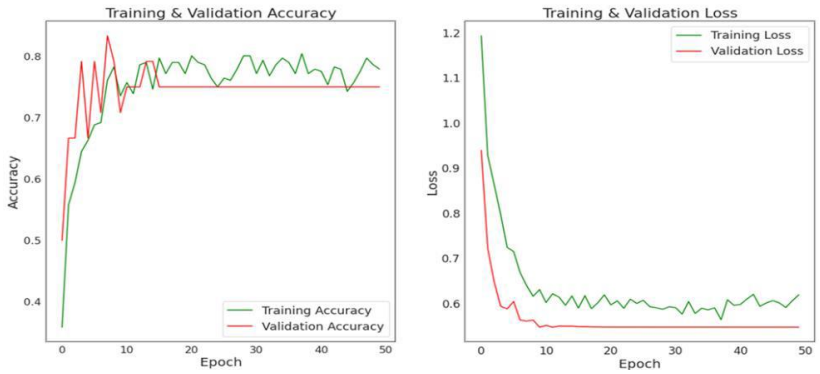

(a) **(b)**

Figure 5: VGG16 Training and Validation for each epoch (a) Model accuracy (b) Model loss.

Figure 6 displays a plot of the training and validation accuracy and loss for the MobileNet architecture for each epoch. Figure 6's learning curves for the MobileNet architecture show that both training and validation loss are getting better, although the two curves are very different from one another. Compared to the validation dataset that was used to assess the problem, this suggests that the model is overfitting and that the training dataset does not include enough information to teach the problem.

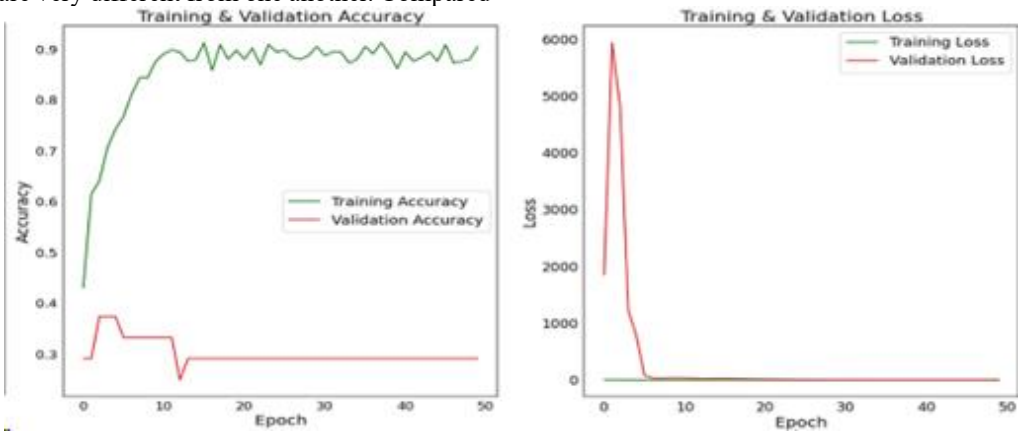

Figure 6: Mobile Net Training and Validation for each epoch (a) Model accuracy (b) Model loss.

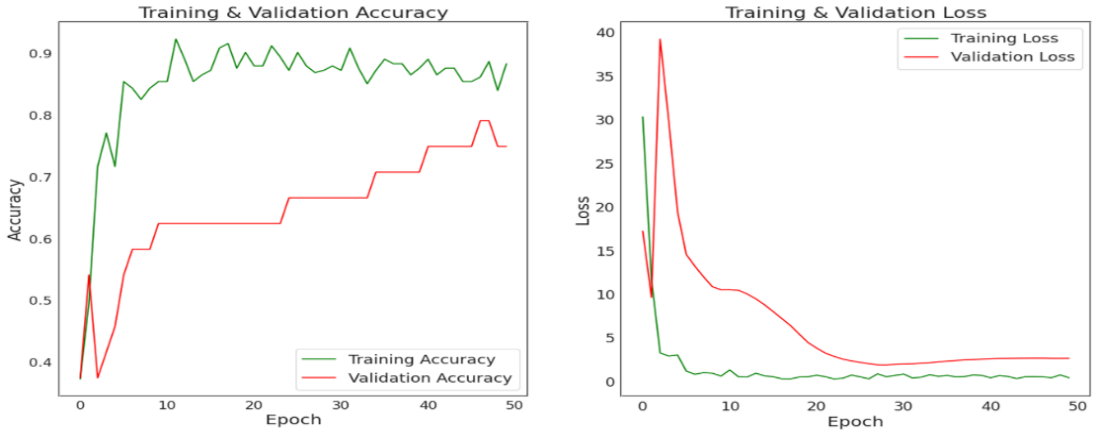

(a) **(b)**

Figure 7: InceptionV3 Training and Validation for each epoch (a) Model accuracy (b) Model loss.

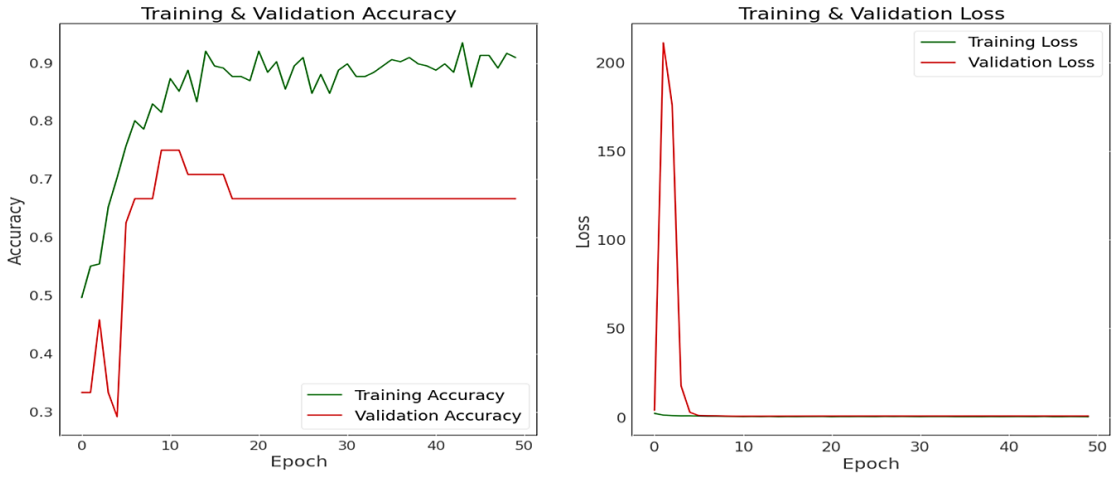

(b) **(b)**

Figure 8: ResNet50 Training and Validation for each epoch (a) Model accuracy (b) Model loss

Figures 7 and 8 display the learning curves for InceptionV3 and ResNet50, respectively. The learning curves show that both models overfit and require additional data to achieve greater generalization. Figure 9 displays the confusion matrices for Mobile Net, VGG16, InceptionV3, and ResNet50. It is evident that nearly all CNNs classify regular instances accurately. There are errors in the other two classes.

This could be because the visual characteristics of the premalignant and malignant groups images coincide. Figure 10 displays the ROC curves for ResNet50, InceptionV3, VGG16, and Mobile Net. As seen in Fig.10, all of the networks—aside from ResNet50, perform exceptionally well in classifying photos into different categories.

To increase performance, these networks can be trained with more photos in subsequent research. An Android device can incorporate a trained network into a mobile application that can be saved and used to analyse captured photos and provide instantaneous findings.

Using artificial intelligence and its variants to computerize the cancer screening procedure is a sensible and helpful way to control oral cancer. This study evaluated the classification accuracy of camera - captured photographs and clinically annotated smartphone photos against gold standard biopsy reports. The present study took into consideration pre - trained CNN models, specifically Mobile Net, VGG19, VGG16, InceptionV3, and ResNet50. Figs.4–7 display the training and testing for each epoch for the models VGG19, VGG16, InceptionV3, and ResNet50, along with the model accuracy, model loss, and confusion matrix. VGG19 performed well out of the five CNN models that were taken into consideration, with an accuracy of 76%. The current study's findings are in favor of creating a low - cost, widely used, and manageable mobile application.

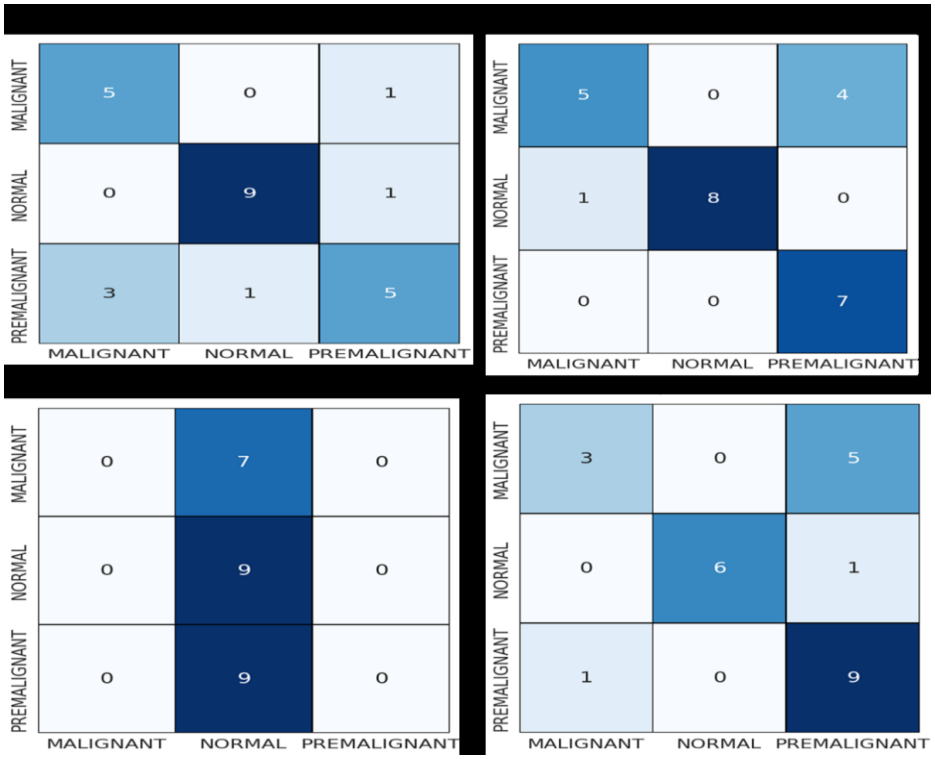

Figure 9: Confusion matrices for Mobile Net, VGG16, InceptionV3 and ResNet50

The main contributing factor to the poor prognosis of oral cancer is the delay in referring patients to cancer specialists. [6] Delays in diagnosis are also caused by a lack of knowledge and experience in recognizing OPMDs and their subtle early indicators. [1] Screening programs conducted by qualified healthcare professionals have been demonstrated to lower mortality, but they have also been described as being more time - consuming, expensive, and physically demanding. [7] Advances in technology such as cox regression models, multifactor analysis, and traditional logistics have enhanced prediction models used in cancer treatment. Similarly, developments in artificial intelligence and related subfields, such as machine learning and deep learning, have opened up new avenues for the diagnosis, treatment, and prognosis of cancer. [14]

The prognosis of oral cancer treatment outcomes has been improved by machine learning algorithms. [15] Tumour infiltration and prognosis estimation have been shown to benefit from deep learning techniques. AI has also been used to discover genes linked to OSCC. [22] However, there is a dearth of data supporting the use of AI for OPMD early detection. Prior research was site - specific, utilizing histological sections or limited to tongue lesions. [23] Using photographic pictures of various oral mucosal locales, our study marks a fresh beginning in which the VGG19 algorithm demonstrates good accuracy in discriminating OPMDs from normal mucosa and OSCC.

Machine learning algorithms have enhanced therapy results prognoses for oral cancer. [15] Deep learning methods have been demonstrated to be beneficial for prognosis assessment and tumour invasion. AI has also been utilized to find genes associated with OSCC. [22] Nevertheless, the application of AI for OPMD early detection is not well supported by data. Previous studies were restricted to tongue lesions or used histological sections for a site - specific approach. [23] Our study represents a new beginning in which the VGG19 algorithm shows good accuracy in differentiating OPMDs from normal mucosa and OSCC using photographic images of different oral mucosal sites. It is applied to scenarios with fewer photos and resources with less processing power. In order to classify photographic images of the oral cavity into three classes normal mucosa, oral possibly malignant diseases, and OSCC therefore take into consideration the transfer learning approach of deep learning. The study employs photographs taken with image - capturing devices such as professional and mobile cameras. Unfortunately, some photographs are too low quality to be used in machine learning, therefore we have to remove them. Therefore, one of the most important criteria in our opinion is the camera's resolution. With the growing application of mobile phones in telemedicine, the usage of these devices as a complement is becoming more common. [25]

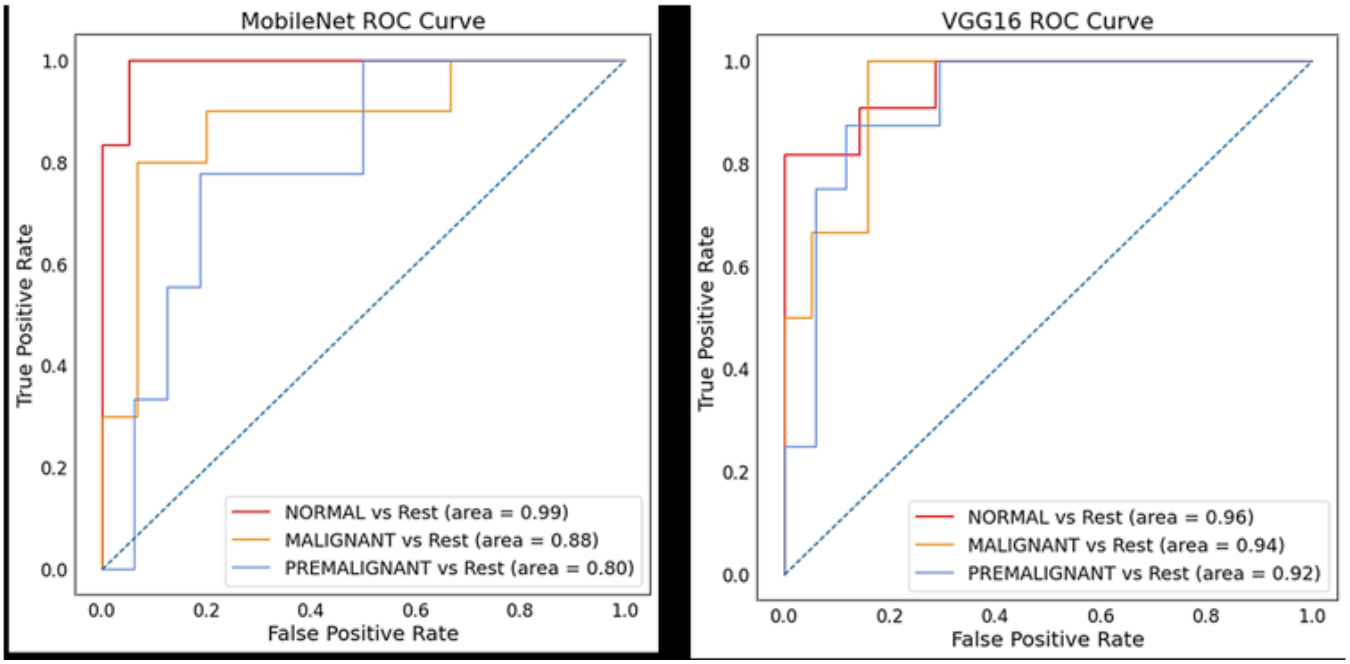

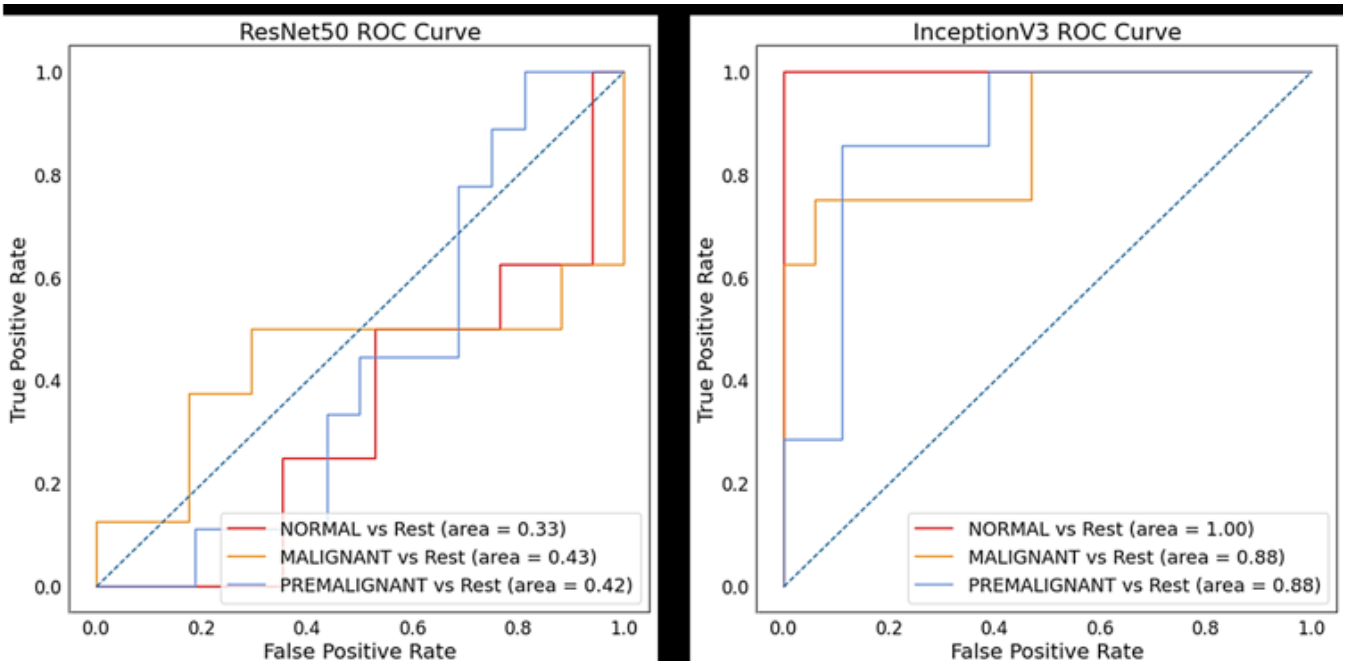

Figure 10: ROC curve for CNN architecture (a) Mobile Net, (b) VGG16, (c) ResNet50, and

(d) InceptionV3.

In order to detect oral cancer, Table 3 presents a summary and comparison of current research that have used transfer learning for categorization. It has been noted that earlier research has utilized images obtained from digital cameras, smartphones, computed tomography (CT), and other sources. [3, 4, 21, 22, 25] While deep learning algorithms are highly effective at categorization, their effectiveness depends on a significant number of datasets. Low - resource environments are not suitable for imaging modalities like magnetic resonance imaging (MRI) and computed tomography (CT). Getting pictures of the mouth cavity using a smartphone is a fairly easy and affordable process. However, there isn't a data set this size available. Therefore, in order to create an effective algorithm, a larger dataset of oral cavity photos with annotations must be developed. Furthermore, different basic ground truth types are employed in different literatures for the construction of algorithms. In earlier research, CNNs performed the best; however, many of these experiments included fewer layers, highlighting the necessity for lightweight networks. When implementing these networks as a mobile application to be integrated into Android smartphones, they are also beneficial. [3, 4, 21, 22, 25, 26]

Table 3 shows that when the quantity of images utilized for learning is increased, CNNs perform better. For this reason, the current study's results are lower than those that have been published. Additionally, the network's performance is greatly influenced by the type of ground truth used, image quality, and feature clarity. Observation reveals that Shamim et al. [21] used a mere 300 photos to achieve an accuracy of 97%. As ground truth, the researchers employed expert annotation and photos of various oral tongue lesions with visually distinguishable features. Images with premalignant and malignant features were not clearly distinguishable. In the current investigation, the diagnosis that was confirmed by a biopsy was taken as gospel. When compared to the accuracy reported by Shamim et al. [21], this could be the cause of the decreased accuracy despite using a comparable number of images.

Table 3: Synopsis and analysis of research with CNN models that have already been trained

Author	Pre-trained CNNs used for experimentation	Number of images	Image type	Ground Truth	CNN which provided the best result	Results
Xu *et al.*[22] 2019	2D CNN 3D CNN	7,000	CT images of early oral cancer	Lableme software	3D CNN	Accuracy: 75.4% Sensitivity: 81.8% Specificity: 73.9%
Welikala *et al.*[4] 2020	ResNet-101	2155	Oral cavity images acquired using smartphones	Expert in the field of Oral Medicine	ResNet-101	Precision: 84.77%, Recall: 89.51% F1 score: 87.07%
Shamim *et al.*[21] 2020	AlexNet, GoogLeNet, Vgg19, ResNet50, Inceptionv3 SqueezeNet	300	Images of the different oral tongue lesions downloaded from the internet	Expert in the field of Oral Medicine	ResNet50	Accuracy: 97% Sensitivity: 89% Specificity: 97%
Jubair *et al.*[3] 2021	EfficientNet-B0 VGG19 ResNet101	716	Tongue images acquired using digital cameras and smartphone	Expert in the field of Oral Medicine	EfficientNet-B0	Accuracy: 85% Specificity: 84.5% Sensitivity: 86.7%
Tanriver *et al.*[25] 2021	ResNet-152, DenseNet-161, Inception-v4, EfficientNet-b4	684	Photographic images of oral lesions	Expert oral pathologist	DenseNet-161	Precision: 87.9%, Recall: 84.1% F1 score: 84.4%
Present Study	MobileNet VGG19 VGG16 InceptionV3 ResNet50	329	Oral cavity images acquired using smartphones	Biopsy	VGG19	Accuracy: 76%

4. Conclusions

The dataset for this study included lesions from the tongue, labial mucosa, and buccal mucosa, and it was unique in that it compared the lesions with the biopsy reports (gold standard). The current study showed how well CNN models performed in identification and classification when compared to a biopsy report. The tiny dataset used in this work is a restriction, however prior research has indicated that CNN models can be strengthened even more by including a wider range of data. More data from various lesions and oral locales is needed for future research in order to automatically identify OSCC and potentially malignant oral illnesses. This work is a step forward in the development of an accurate and reasonably priced oral cancer screening tool.

5. Future Scope

To achieve better performance, the network must be trained and optimized using a larger dataset. Utilizing the trained network and releasing it as a mobile application that can be integrated into an Android or iOS device are two areas of future development. The mobile application can be used to evaluate the obtained photographs and provide an immediate result. This would facilitate the prompt identification of oral cancer in remote areas where access and knowledge are limited.

References

[1] B. Ilhan, P. Guneri, P. Wilder - Smith, *Oral Oncology*, 2021, **116**, 105254, doi: 10.1016/j. oraloncology.2021.105254.

[2] H. Sung, J. Ferlay, R. L. Siegel, M. Laversanne, I. Soerjomataram, A. Jemal, F. Bray, *CA: A Cancer Journal for Clinicians*, 2021, **71**, 209 - 249, doi: 10.3322/caac.21660.

[3] F. Jubair, O. Al - karadsheh, D. Malamos, S. Al Mahdi, Y. Saad, Y. Hassona, *Oral Diseases*, 2022, **28**, 1123 - 1130, doi: 10.1111/odi.13825.

[4] R. A. Welikala, P. Remagnino, J. H. Lim, C. S. Chan, S. Rajendran, T. G. Kallarakkal, R. B. Zain, R. D. Jayasinghe, J. Rimal, A. R. Kerr, R. Amtha, K. Patil, W. M. Tilakaratne, J. Gibson, S. C. Cheong, S. A. Barman, *IEEE Access*, 2020, **8**, 132677 - 132693, doi: 10.1109/ACCESS.2020.3010180.

[5] S. Warnakulasuriya, N. W. Johnson, I. van der Waal, *Journal of Oral Pathology & Medicine*, 2007, **36**, 575 - 580, doi: 10.1111/j.1600 - 0714.2007.00582. x.

[6] H. Mahmood, M. Shaban, B. I. Indave, A. R. Santos - Silva, N. Rajpoot, S. A. Khurram, *Oral Oncology*, 2020, **110**, 104885, doi: 10.1016/j. oraloncology.2020.104885.

[7] Q. Fu, Y. Chen, Z. Li, Q. Jing, C. Hu, H. Liu, J. Bao, Y. Hong, T. Shi, K. Li, H. Zou, Y. Song, H. Wang, X. Wang, Y. Wang, J. Liu, H. Liu, S. Chen, R. Chen, M.

Zhang, J. Zhao, J. Xiang, B. Liu, J. Jia, H. Wu, Y. Zhao, L. Wan, X. Xiong, *EClinicalMedicine*, 2020, **27**, 100558, doi: 10.1016/j. eclinm.2020.100558.

[8] M. Petruzzi, M. de Benedittis, *Oral Surgery, Oral Medicine, Oral Pathology and Oral Radiology*, 2016, **121**, 248 - 254, doi: 10.1016/j. oooo.2015.11.005.

[9] N. Haron, R. B. Zain, W. M. Nabillah, A. Saleh, T. G. Kallarakkal, A. Ramanathan, S. H. M. Sinon, I. A. Razak, S. C. Cheong, *Telemedicine and e - Health*, 2017, **23**, 192 - 199, doi: 10.1089/tmj.2016.0128.

[10] K. Vinayagamoorthy, S. Acharya, M. Kumar, K. C. Pentapati, S. Acharya, *Australian Journal of Rural Health*, 2019, **27**, 170 - 176, doi: 10.1111/ajr.12496.

[11] A. Esteva, B. Kuprel, R. A. Novoa, J. Ko, S. M. Swetter, H. M. Blau, S. Thrun, *Nature*, 2017, **542**, 115 - 118, doi: 10.1038/nature21056.

[12] S. Attardo, V. T. Chandrasekar, M. Spadaccini, R. Maselli, H. K. Patel, M. Desai, A. Capogreco, M. Badalamenti, P. A. Galtieri, G. Pellegatta, A. Fugazza, S. Carrara, A. Anderloni, P. Occhipinti, C. Hassan, P. Sharma, A. Repici, *World Journal of Gastroenterology*, 2020, **26**, 5606 - 5616, doi: 10.3748/wjg. v26. i37.5606.

[13] Y. LeCun, Y. Bengio, G. Hinton, *Nature*, 2015, **521**, 436 - 444, doi: 10.1038/nature14539.

[14] P. R. Jeyaraj, E. R. Samuel Nadar, *Journal of Cancer Research and Clinical Oncology*, 2019, **145**, 829 - 837, doi: 10.1007/s00432 - 018 - 02834 - 7.

[15] M. Aubreville, C. Knipfer, N. Oetter, C. Jaremenko, E. Rodner, J. Denzler, C. Bohr, H. Neumann, F. Stelzle, A. Maier, *Scientific Reports*, 2017, **7**, 11979, doi: 10.1038/s41598 - 017 - 12320 - 8.

[16] M. Aubreville, C. Knipfer, N. Oetter, C. Jaremenko, E. Rodner, J. Denzler, C. Bohr, H. Neumann, F. Stelzle, A. Maier, *Scientific Reports*, 2017, **7**, 11979, doi: 10.1038/s41598 - 017 - 12320 - 8.

[17] T. Y. Rahman, L. B. Mahanta, A. K. Das, J. D. Sarma, *Tissue and Cell*, 2020, **63**, 101322, doi: 10.1016/j. tice.2019.101322.

[18] P. H. Chen, R. Shimada, S. Yabumoto, H. Okajima, M. Ando, C. T. Chang, L. T. Lee, Y. K. Wong, A. Chiou, H. O. Hamaguchi, *Scientific Reports*, 2016, **6**, 20097, doi: 10.1038/srep20097.

[19] R. Anantharaman, V. Anantharaman, Y. Lee, *2017 IEEE International Conference on Healthcare Informatics (ICHI)*, 2017, 39 - 45, doi: 10.1109/ICHI.2017.69.

[20] R. Anantharaman, M. Velazquez, Y. Lee, *2018 IEEE International Conference on Bioinformatics and Biomedicine (BIBM)*, 2018, 2197 - 2204, doi: 10.1109/BIBM.2018.8621112.

[21] M. Z. M, Shamim, S. Syed, M. Shiblee, M Usman, S. Ali, *arXiv*, 1909, 08987, doi: 10.48550/arXiv.1909.08987.

[22] S. Xu, C. Liu, Y. Zong, S. Chen, Y. Lu, L. Yang, E. Y. K. Ng, Y. Wang, Y. Wang, Y. Liu, W. Hu, C. Zhang, *IEEE Access*, 2019, **7**, 158603 - 158611, doi: 10.1109/ACCESS.2019.2950286.

[23] A. S. Sultan, M. A. Elgharib, T. Tavares, M. Jessri, J. R. Basile, *Journal of Oral Pathology & Medicine*, 2020, **49**, 849 - 856, doi: 10.1111/jop.13042.

[24] M. Z. M. Shamim, S. Syed, M. Shiblee, M. Usman, S. J. Ali, H. S. Hussein, M. Farrag, *The Computer Journal*, 2022, **65**, 91 - 104, doi: 10.1093/comjnl/bxaa136.

[25] G. Tanriver, M. Soluk Tekkesin, O. Ergen, *Cancers*, 2021, **13**, 2766, doi: 10.3390/cancers13112766.

[26] V. Patil, R. Vineetha, S. Vatsa, D. K. Shetty, A. Raju, N. Naik, N. Malarout, *Cogent Engineering*, 2020, **7**, 1723783, doi: 10.1080/23311916.2020.1723783.